ORIGINAL ARTICLE

Wild type but not mutant APP is involved in protective adaptive responses against oxidants

Giovanna Cenini · Giuseppina Maccarinelli · Cristina Lanni · Sara Anna Bonini · Giulia Ferrari-Toninelli · Stefano Govoni · Marco Racchi · David Allan Butterfield · Maurizio Memo · Daniela Uberti

Abstract This study points out different behaviour between HEK cells overexpressing wild-type or mutant APP when exposed to oxidative insult. Although apparently both APPwt and APPmut overexpression conferred resistance to oxidative insult, some differences in terms of degree of protection was observed in the two clones. We found that the two clones differed, especially, in terms of redox profile. HEK-APPmut cells were characterized by higher levels of oxidative markers in comparison with HEK-APPwt. In addition, SOD activity appeared more efficient in HEK-APPwt than in HEK-APPmut, thus justifying the differences in terms of cell survival in the two clones. We suggest that, according to "hormesis theory", in HEK-APPwt cells low amount of oxidative stress can exert a beneficial effect that at a higher intensity results harmful. In contrast, HEK-APPmut cells lost this stress resistance probably because the degree of oxidative stress is too high and the antioxidant enzymes are themselves compromised.

G. Cenini · G. Maccarinelli · S. A. Bonini ·
G. Ferrari-Toninelli · M. Memo · D. Uberti (✉)
Department of Biomedical Sciences and Biotechnologies,
University of Brescia, Viale Europa 11, 25123 Brescia, Italy
e-mail: uberti@med.unibs.it

C. Lanni · S. Govoni · M. Racchi
Department of Experimental and Applied Pharmacology,
University of Pavia, Pavia, Italy

G. Cenini · D. A. Butterfield
Sanders-Brown Centre on Aging, University of Kentucky,
Lexington, KY, USA

M. Memo
National Institute of Neuroscience, University of Torino,
Torino, Italy

Introduction

Amyloid precursor protein (APP) is a type I membrane-spanning glycoprotein expressed in a wide variety of tissue and cell types. At least 10 isoforms of the protein derived by alternative splicing have been described with the 695, 751 and 770 amino acid isoforms being the most common. APP695 is expressed only in neurons, whereas the other forms are present in many other cell types. The two longer forms of the molecule contain a Kunitz-type serine protease inhibitor domain (KIP) which is coded by exon 7 (168 nucleotides) of the APP gene. APP undergoes intensive processing and its metabolic products have different effects. In the amyloidogenic pathway, APP can be subsequently cleaved by β-secretase and γ-secretase, resulting in Aβ peptides and an APP intracellular domain, which is also known as carboxy terminal segment ε (CTSε). In the non-amyloidogenic pathway, APP is first processed by α-secretase within the Aβ sequence to produce sAPPα and a membrane-associated carboxy terminal segment α (CTFα), which undergoes further γ-secretase processing to result in the formation of p3 and CTSε (De Strooper and Annaert 2000; Vetrivel and Thinakaran 2006; LaFerla et al. 2007; Walsh et al. 2007; Thinakaran and Koo 2008). So far, the pathophysiological role of APP and its proteolytic fragments, including Aβ peptides, have mainly been considered as being brain specific (Pearson and Peers 2006; Walsh and Selkoe 2007; Knobloch and Mansuy 2008; Selkoe 2008). Abnormal generation and accumulation of Aβ peptides in brain is thought to be one of the causative events in Alzheimer's disease (AD) (Shankar et al. 2008).

The amyloid hypothesis in AD is sustained by the identification of gene mutations in familial cases of the pathology. AD-related mutations specifically affect γ-secretase-mediated processing, with an accumulation of $A\beta$ peptides, especially the 42 amino acids length fragment. However, the ubiquitous production of APP and $A\beta$ peptides indicates that their functions are also ubiquitous (Graebert et al. 1995; Schmitz et al. 2002; Grimm et al. 2007). Recently, the APP751 isoform, which is expressed mainly in non-neuronal cells, has been demonstrated to undergo an intense amyloidogenic metabolism with production of $A\beta$ fragments. Furthermore, numerous studies reported different effects of APP metabolic products in non-neuronal cells (Beer et al. 1995; Herzog et al. 2004). For example, in epithelial cells, APP metabolism has been found to increase cell proliferation and cell migration (Schmitz et al. 2002). APP metabolic products have also been shown to stimulate cell division in APP-deficient fibroblasts (Saitoh et al. 1989). Moreover, nanomolar concentrations of $A\beta$ peptides activate angiogenesis by promoting endothelial cell proliferation and migration as well as pseudocapillary formation on microvascular endothelial cells (Cantara et al. 2004). Xu et al. (1999), showed that wild type (wt), but not mutant (mut) APP effectively protected neuroblastoma cells against apoptosis induced by ultraviolet irradiation and staurosporine. Moreover, we recently demonstrated that overexpression of APP751 rendered HEK cells less sensitive to doxorubicin insult (Uberti et al. 2007). Interestingly, in these clones cell resistance upon cytotoxic insult was recapitulated by γ and β secretase inhibitors, but not by α secretase inhibitor, suggesting a role for $A\beta$ peptides in such effect (Uberti et al. 2007).

Here, we describe the redox profile of HEK cells overexpressing wild type APP (HEK-APPwt) or mutant APP (HEK-APPmut) and demonstrate how the different redox state can influence the response of the two experimental cell lines to a toxic acute oxidative insult. Furthermore, the different behaviour of HEK-APPwt and HEK-APPmut was discussed in light of the effects of $A\beta_{1-40}$ and $A\beta_{1-42}$ peptide treatments.

Materials and methods

Cell culture and transfections

HEK-293 cells were cultured in Dulbecco's modified Eagle's medium (Sigma-Aldrich, St Louis, MO, USA) containing 10% foetal bovine serum (Sigma-Aldrich, St Louis, MO, USA), 2 mM glutamine (Sigma-Aldrich), 100 units/ml penicillin (Sigma-Aldrich) and 100 µg/ml

streptomycin (Sigma-Aldrich) at 37°C in a 5% CO_2-containing atmosphere.

The HEK-293 cell stable transfection with APP 751 wild type (HEK-APPwt) and APP (val717gly) mutation (HEK-APPmut), was prepared as follows. HEK-293 cells, seeded on polylysine-coated 6-well plate at 80% of confluence density were transfected with 1 µg/well of pcDNA–APP751 vector or 1 µg/well of pcDNA–APP751 (val717gly) mutation vector using Lipofectamine™ 2000 reagent (Invitrogen, Milan, Italy). G418 (Sigma-Aldrich) was added at a concentration of 800 µg/ml and drug resistant cells were collected after 2–3 weeks for single cell cloning; transfected cells were diluted, and seeded in 96-well plates at one cell per well. Wells that contained more than one cell were marked and excluded from further investigation. As much as 50% of the medium in each well was replaced twice a week. After 4–6 weeks, surviving clones reached confluency and were expanded for banking. Resistant clones were analysed by Western blot to confirm the overexpression of APP. Stable transfected cells expressing the APPwt or APPmut construct were maintained in G418 at a final concentration of 300 µg/ml.

$A\beta$ treatment

$A\beta_{1-40}$ and $A\beta_{1-42}$, were purchased from Invitrogen S.R.L. (San Giuliano Milanese (MI), Italy). The peptides were solubilized in DMSO at the concentration of 1 mM and frozen in stock aliquots. Stock aliquots were diluted at the final concentration of 10 nM prior to use. All the experiments performed with $A\beta$ were made in 1% of serum.

H_2O_2 pulse

Cells were used at 80% confluent monolayers and they were exposed to 1 mM H_2O_2 (Sigma-Aldrich) pulse for 5 min; then the H_2O_2 containing medium was replaced with full medium and incubated for additional different times: 30′, 1 h, 4 h and 24 h according to the designed experiments.

Cell viability

Cell viability was measured by quantitative colorimetric assay with MTT (3-(4,5-dimethylthiazol-2-yl)-2,5-diphenyltetrazolium bromide) (Sigma-Aldrich), showing the mitochondrial activity of living cells. HEK clones in 96-well plates were exposed to 1 mM H_2O_2 pulse for 5 min; then the H_2O_2 containing medium was replaced with full medium and incubated for an additional 24 h. At the end of this incubation time, 500 µg/ml MTT

(final concentration) was added to well and cells were incubated at 37°C for 3 h. MTT was removed, and cells were lysed with dimethyl sulfoxide (DMSO, Sigma-Aldrich). The absorbance at 595 nm was measured using a Bio-Rad 3350 microplate reader. Control cells were treated in the same way without H_2O_2 pulse, and the values of different absorbances were expressed as a percentage of control.

Western blot analysis

Proteins were extracted from the cells as previously described (Uberti et al. 2002) and proteins content were determined by a conventional method (BCA protein assay Kit, Pierce, Rockford, IL). As much as 30 μg of protein extracts were electrophoresed on 12% SDS-PAGE, and transferred to nitrocellulose paper (Amersham-GE Life Sciences Healthcare, Milan, Italy). Filters were incubated at room temperature overnight with primary antibodies in 5% non-fat dried milk (Euroclone CELBIO, Milan, Italy). The antibodies used for this study were: the antibody that recognized the N-terminus domain of APP protein (2C11, 1:150, Chemicon-Millipore, Billerica, MA, USA), antibodies that recognize the two isoforms of superoxide dismutase, Cu–Zn superoxide dismutase (anti-SOD1, 1:400, Santa Cruz Biotechnology Inc., Heidelberg, Germany), and Mn-superoxide dismutase (anti-SOD2, 1:300 Sigma-Aldrich, St Louis, MO, USA), the antibody anti-p53 (CM1, 1:1000, Novocastra, Newcastle, UK), the antibody anti-p21/WAF1 (1:200, Santa Cruz Biotechnology Inc., Heidelberg, Germany) and anti-α-tubulin antibody (1:1.500, Sigma-Aldrich, St Louis, MO, USA). The secondary antibodies (Dako, Glostrup, Denmark) and a chemiluminescence blotting substrate kit (Amersham-GE Life Sciences Healthcare, Milan, Italy) were used for immunodetection. Evaluation of immunoreactivity was performed on immunoblots by densitometric analysis using Scion Image (PC version of Macintosh-compatible NIH Image) software.

Measurement of protein carbonyls

Protein carbonyls are an index of protein oxidation and were determined as described in Prof. Butterfield's laboratory (Butterfield and Stadtman 1997) Briefly, samples (5 μl of proteins) were derivatized with 10 mM 2,4-dinitrophenylhydrazine (DNPH) (from OxyBlot[tm] Protein oxidation Detection Kit, Chemicon International), in the presence of 5 μl of 12% sodium dodecyl sulphate for 20 min at room temperature (23°C). The samples were then neutralized with 7.5 μl of the neutralization solution (2 M Tris in 30% glycerol). Derivatized protein samples were then blotted onto a nitrocellulose membrane with a dot-blot apparatus (2 μg per dot). The membrane was blocked with

a solution of 5% non-fat dried milk in Tris-buffered saline (TBS) solution and followed by incubation with rabbit polyclonal anti-DNPH antibody (1:100 dilution, from OxyBlot[tm] Protein oxidation Detection Kit, Chemicon-Millipore, Billerica, MA, USA) as primary antibody for 1 h at room temperature. After washing the membrane with TBS buffer, it was further incubated with HRP-conjugated goat anti-rabbit antibody (1:300, from OxyBlot[tm] Protein oxidation Detection Kit, Chemicon-Millipore, Billerica, MA, USA) as secondary antibody for 1 h at room temperature. Blots were developed using chemiluminescence blotting substrate kit (Amersham-GE Life Sciences Healthcare, Milan, Italy), scanned with Adobe Photoshop, and quantified using Scion Image (PC version of Macintosh-compatible NIH Image) software. Non-specific binding of the primary or secondary antibodies was found.

Measurement of 3-nitrotyrosine (3-NT)

Nitration of proteins is another form of protein oxidation (Castegna et al. 2003). The nitrotyrosine content was determined immunochemically as previously described (Drake et al. 2003). Briefly, samples were incubated with Laemmli sample buffer in a 1:2 ratio (0.125 M Trizma base, pH 6.8, 4% sodium dodecyl sulphate, 20% glycerol) for 20 min. Proteins (5 μg) were then blotted onto the nitrocellulose paper using the slot-blot apparatus and immunochemical methods as described above for protein carbonyls. The rabbit anti-nitrotyrosine antibody (1:1000 dilution) (Sigma-Aldrich, St Louis, MO, USA) at 4°C over night and at room temperature for 3 h was used as the primary antibody and HRP-conjugated goat anti-rabbit antibody (1:1500, Dako, Glostrup, Denmark) at room temperature for 2 h was used for detection. Blots were then scanned by Adobe Photoshop program, and densitometric analysis of bands in images of the blots was used to calculate levels of 3-NT. A small background of the primary antibody binding to the membrane was found, but this was scattered from both control and subject blots.

Measurement of 4-hydroxynonenal (HNE)

HNE is a marker of lipid oxidation and the assay was performed as previously described (Lauderback et al. 2001). Briefly, 10 μl of sample was incubated with 10 μl of Laemmli buffer containing 0.125 M Tris base, pH 6.8, 4% (v/v) SDS and 20% (v/v) glycerol. The resulting sample (5 μg) was loaded per well in the slot-blot apparatus containing a nitrocellulose membrane under vacuum pressure. The membrane was blocked with a solution of 5% non-fat dried milk in Tris-buffered saline (TBS) solution and incubated with a 1:200 dilution of anti-4-hydroxynonenal (HNE) polyclonal antibody (Alpha diagnostic, Vinci-Biochem,

Vinci, Italy) at 4°C over night and 3 h at room temperature. An anti-rabbit IgG alkaline phosphatase secondary antibody (Dako, Glostrup, Denmark) was diluted 1:1,500 in a solution of 5% non-fat dried milk in Tris-buffered saline (TBS) solution and added to the membrane for 2 h at room temperature. Blots were dried, scanned with Adobe Photoshop program and quantified by Scion Image. A small background of the primary antibody binding to the membrane was found, but this was scattered from both control and subject blots.

Superoxide dismutase activity

SOD total was measured using a buffer (G buffer) that contained 0.05 M glycine, 0.1 M NaOH and 0.1 M NaCl, pH 10.3 and epinephrine. The reaction was monitored in a 96-well plate reader by measuring the decrease of absorbance at 480 nm.

p21 Transactivation assay

As much as 1 μg of p21-luc plasmid (gifted by Varda Rotter, Weizmann, Israel) was transfected into HEK, HEK-APP cells and HEK-APPmut cells. After 24 h the cells were treated with 1 mM H_2O_2 pulse for 5 min. After 4 h cell lysates were harvested and assayed for luciferase activity using the Dual Luciferase Reporter Assay System (Promega, Madison, WI, USA) and a 1450 microbeta Trilux counter (Perkin Elmer, MA, USA). In all experiments, cell extracts were equalized for total proteins.

ROS production in mitochondria

Mitochondrial ROS production was analysed in real time by a video-rate confocal microscopy-based method. Briefly, cells were plated in wells with glass dish and after 24 h resuspended in physiological buffer containing the ROS Detection Reagent (CM-H_2CFDA) at the final concentration of 1 μM. Cells were also loaded with Mitotracker Deep Red 633 FM (100 nM) (Invitrogen, Milan, Italy) for 45′ in 5% CO_2 at 37°C for mitochondrial localization. Oxidative insult was performed exciting the cells at increasing laser intensity (from 4% to 9%) and CM-DCF fluorescence intensity was selectively recorded in mitochondria. Fluorescence emission intensity was calculated as average green level value per pixel and corrected for background.

Immunoprecipitation analysis

To analyse p53 conformation, cells were lysed in immunoprecipitation buffer (10 mM Tris, pH 7.6; 140 mM NaCl; and 0.5% NP40 including protease inhibitors) for 20 min on ice, and cell debris was cleared by centrifugation. Protein content was determined by a conventional method (BCA protein assay Kit, Pierce, Rockford, IL). Before immunoprecipitation experiments, an aliquot of 10 μg of protein extracts from each individual sample was processed for Western blot analysis and probed with anti-β tubulin antibody to validate protein content measurements (data not shown). Based on the previous results, 100 μg of protein extracts were used for immunoprecipitation experiments performed in a volume of 500 μl. To prevent non-specific binding, the supernatant of immunoprecipitated samples was pre-cleared with 10% (w/v) protein A/G (50 μl) (Santa Cruz Biotechnology Inc., Heidelberg, Germany) for 20 min on ice, followed by centrifugation. For immunoprecipitation of p53, 1 μg of the conformation-specific antibodies PAb1620 (wild-type specific) (Calbiochem, EMB Bioscience, La Jolla, CA, USA), PAb240 (mutant specific) (Neomarkers-Lab Vision, Fremont, CA, USA) or PAbBP53.12 (Neomarkers-Lab Vision, Fremont, CA, USA) (recognizing both wild-type and mutant p53) were added to the samples overnight at 4°C. Immuno-complexes were collected by using protein A/G suspension and washed 5 times with immunoprecipitation buffer. Immunoprecipitated p53 was recovered by resuspending the pellets in Laemmli sample buffer. Western blot was performed using as primary antibody the polyclonal anti-p53, antibody CM1 (Novocastra, Newcastle, UK) at a 1:1,000 dilution, anti-HNE and anti-3NT antibodies mentioned above.

Reactive oxygen species detection

Detection of intracellular ROS was performed as previously described (Uberti et al. 2007): cell cultures grown on 35-mm dishes were incubated with 10 μM 2′,7′-dichlorofluorescin (DCF) diacetate (Molecular Probes, Eugene, OR, USA) for 30 min at 37°C after a time course with different $A\beta$ species. The cells were then rinsed with Kreb's ringer solution. Intracellular esterases convert DCF diacetate to anionic DCFH which is trapped in the cells. The fluorescence of DCF, formed by the reaction of DCFH with ROS was examined with Fusion TM Master (Packard Bioscience Company).
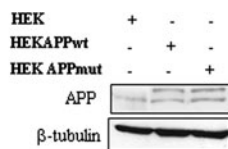
Statistical evaluation

Results are expressed as mean values ± standard error. Statistical significance of differences was determined by mean values of the one way ANOVA, followed by Bonferroni test. Significance was accepted for a p value < 0.05.

Results

Characterization of HEK-APPwt and HEK-APPmut cells

In our laboratory, several clones of cells overexpressing wt or mutant APP were developed. The choice of the two clones used for the present study was limited by their ability to express comparable APP levels. Thus, HEK-APPwt and HEK-APPmut cells were first characterized for APP overexpression (Fig. 1, upper panel) and $A\beta$ peptide load (Fig. 1, lower panel). As reported in a representative Western blot, the two clones, stable transfected with either APPwt or APPmut, expressed similar APP levels and higher than those found in non-transfected cells (Fig. 1, upper panel). $A\beta_{1-40}$ and $A\beta_{1-42}$ were measured using an ELISA kit in cell extracts and cell media. HEK-APPwt expressed and released into the medium a higher amount of $A\beta_{1-40}$, while HEK-APPmut expressed and released predominantly the 42-length peptide. The calculated ratio $A\beta_{1-42}/A\beta_{1-40}$ values were significantly higher in HEK-APPmut cells in comparison with HEK-APPwt clone both in the medium and cellular extracts.

HEK-APPwt, HEK-APPmut and non-transfected cells were then exposed to a toxic oxidative injury. In particular, the two clones and non-transfected cells were challenged for a brief period of time with 1 mM H_2O_2; then H_2O_2 medium was replaced with fresh medium and cells were incubated for an additional 24 h. After that period of time, the MTT assay was performed. Results reported in Fig. 2 show that a H_2O_2 pulse to non-transfected cells caused about 50% cell death. Overexpression of wt or mut APP rendered the cells less sensitive to H_2O_2. As shown in

Fig. 1 Characterization of HEK-APPwt and HEK-APPmut cells. *Upper panel* Western blot analysis of total cellular extracts from HEK, HEK-APPwt and HEK-APPmut cells was performed with monoclonal 2C11 antibody. Tubulin expression was used to normalize the samples. *Lower panel* levels of $A\beta_{1-40}$ and $A\beta_{1-42}$ peptides were measured with a commercial ELISA kit in the cellular extracts and conditioned media of HEK-APPwt and HEK-APPmut cells. Values are expressed as mean ± SEM of at least 3 different experiments
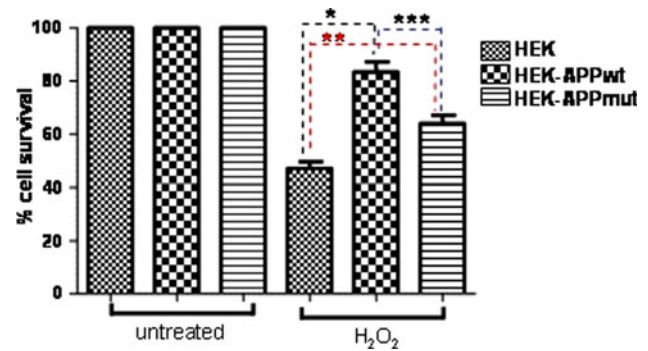
SAMPLES	$A\beta_{1-42}$	$A\beta_{1-40}$	$A\beta_{1-42}/A\beta_{1-40}$	$A\beta_{1-42}$	$A\beta_{1-40}$	$A\beta_{1-42}/A\beta_{1-40}$
	Medium (pg/ml)			Cell extracts (pg/mg proteins)		
HEK-APP wt	310	480	0,64	96	230	0,41
HEK-APP mut	500	290	1,7	153	120	1,3

Fig. 2 Sensitivity of HEK, HEK-APPwt and HEK-APPmut cells to oxidative insult. HEK, HEK-APPwt and HEK-APPmut cells were treated for 5 min with 1 mM H_2O_2, and then replaced with fresh medium. After incubation of the cells for additional 24 h, the cell vulnerability was measured by MTT assay. The data were expressed as % of cell survival versus control. Values are expressed as mean ± SEM of at least 3 different experiments. *$p < 0.01$ HEK-APPwt versus corresponding control, **$p < 0.01$ HEK-APPmut versus corresponding control, ***$p < 0.05$ HEK-APPmut versus HEK-APPwt

Fig. 2, the cytotoxic effects induced by H_2O_2 were significantly reduced in both APP-transfected cells, leading to about 20% of cell death in HEK-APPwt and 40% of cell death in HEK-APPmut cells. The different response of the APP-transfected cells was statistically significant ($p < 0.05$ HEK-APPwt vs. HEK-APPmut), indicating that HEK-APPmut cells are more sensitive to an oxidative insult in comparison with HEK-APPwt.

p53 intracellular signalling in HEK-APPwt and HEK-APPmut

Among death pathways activated by ROS, the p53 intracellular signalling is one of the most characterized (Johnson et al. 1996; Gansauge et al. 1997; Uberti et al. 1999; Nakamura and Sakamoto 2001). Here, we studied p53 signalling by measurement of protein levels, transcriptional activity and its conformational state in HEK-APPwt, HEK-APPmut and non-transfected cells. In non-transfected cells H_2O_2 exposure caused an increase of p53 levels at 30 min, which declined at 4 h (Fig. 3, panel A). Induction of p53 in non-transfected cells was followed by transcriptional activation of p21/waf1 luciferase promoter (Fig. 3, panel B) and increased expression of p21/waf1 protein (Fig. 3, panel A). This is a well-characterized pattern of p53 pathway response observed in many cell phenotypes. In contrast, in HEK-APPwt, p53 was already high in basal condition, and H_2O_2 treatment did not induce any significant change, while in HEK-APPmut oxidative injury induced a slight increase of p53 that was evident at 1 h after the insult (Fig. 3, panel A). On the other hand, independently from the p53 response in the two clones, p53 intracellular
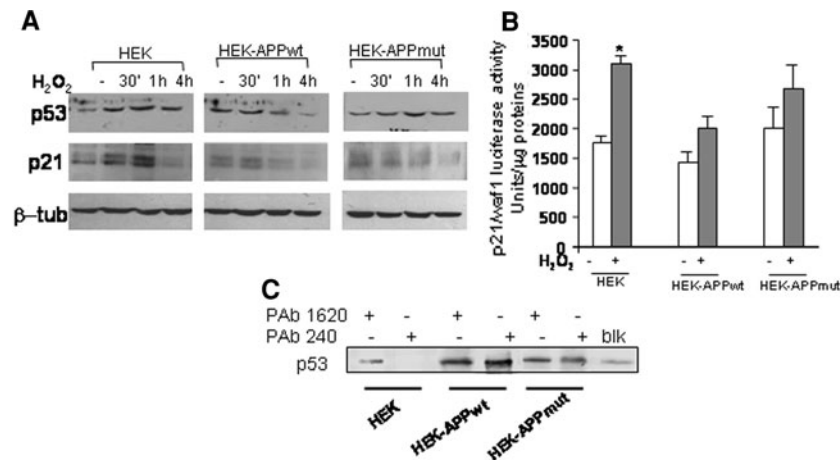
Fig. 3 p53 intracellular signal in HEK, HEK-APPwt and HEK-APPmut cells. **a** HEK, HEK-APPwt cells and HEK-APPmut cells were treated for 5 min with H_2O_2 1 mM, followed by incubation with fresh medium for different times (30′, 1 h, 4 h). p53 and p21/waf1 expression were evaluated by Western blotting analysis with specific antibodies as described in "Materials and methods" section. Tubulin expression was used to normalize the samples. **b** HEK, HEK-APPwt and HEK-APPmut cells were transfected with p21 luc-promoter and 24 h later they were treated with H_2O_2. As much as 4 h after H_2O_2 pulse, cells were processed for measurement of luciferase activity. Data were expressed as luciferase activity over μg proteins. *$p < 0.01$ H_2O_2 treated HEK versus corresponding control. **c** Protein extracts derived from HEK, HEK-APPwt and HEK-APPmut cells were immunoprecipitated with the following antibodies: PAb240 (specific for "mutant" unfolded conformation) and PAb1620 (specific for wild-type folded conformation). Immunoprecipitates were analysed by Western blot with the CM1 polyclonal anti-p53 antibody

signalling was compromised in both clones, as shown by lack of increased transcriptional activation of p21/waf1 luciferase promoter (Fig. 3, panel B) and p21/waf1 protein expression (Fig. 3, panel A) after H_2O_2 injury. Finally, HEK-APPwt and HEK-APPmut expressed a "mutant like" p53 isoform, recognized by PAb 240 antibody, which binds to an epitope that is masked when the protein is in the wt conformation and is revealed when the protein is in unfolded tertiary structure. A PAb 1620-positive p53 band representing the p53 wild type isoform, is also present in the two clones and non-transfected cells (Fig. 3, panel C).

Oxidative profile in HEK-APPwt
and HEK-APPmut cells

HEK-APPwt and HEK-APPmut cells were compared in terms of redox profile. As an index of redox state, we evaluated the levels of different oxidative markers, which are the final products of oxidation and nitrosylation processes. In particular, we focused on protein-bound 4-hydroxy-2-nonenal (HNE), which is one of the main products of lipid peroxidation (Markesbery and Lovell 1998; Butterfield et al. 2002; Uchida 2003); 3-nitrotyrosine (3NT), which, via peroxynitrite, results in the addition of a nitro group to tyrosine residues, and protein carbonyls (PC), which is an established indicator of ROS-mediated protein oxidation (Butterfield and Stadtman 1997; Castegna et al. 2003; Sultana et al. 2006°, 2006b, 2009).

HNE, 3NT and PC products were measured in HEK-APPwt and HEK-APPmut cells by using dot-blot technique (Butterfield et al. 2006; Perluigi et al. 2006; Sultana and Butterfield 2008). The results are shown in Fig. 4. Protein-bound HNE and 3NT levels were significantly higher in HEK-APPmut in comparison to HEK-APPwt cells (Fig. 4, panels A and B). Protein-bound HNE and 3NT levels in HEK-APPwt were, also, higher than those found in HEK non-transfected cells (Fig. 4, panels A and B). PC levels were found increased in HEK-APPwt and HEK-APPmut in comparison with HEK non-transfected cells, however, no differences in terms of PC markers were observed between HEK-APPwt and HEK-APPmut (Fig. 4, panel C).

As an additional index of cell redox state, we evaluated mitochondrial ROS levels using confocal microscopy technology in living cells after exposure to increasing laser light intensity. This technique has been well recognized to cause an oxidative damage (Dugan et al. 1995; Kweon et al. 2001; Alexandratou et al. 2005). In HEK-APPmut cells, increasing light intensity was associated with increased mitochondrial ROS generation (green fluorescence). On the other hand, HEK-APPwt mitochondria produced a very low amount of ROS in comparison with HEK-APPmut cells, at each laser intensity examined (Fig. 5).

Antioxidant enzymes contribute to the assessment of the oxidative profile of cells (Valko et al. 2007). Increased oxidative stress is, in fact, the result of imbalance between oxidants and antioxidants (Gutteridge and Halliwell 2000; Halliwell 2007, 2009). Thus, we evaluated the enzyme activity and protein expression of superoxide dismutase (SOD), which is one of the most important antioxidant
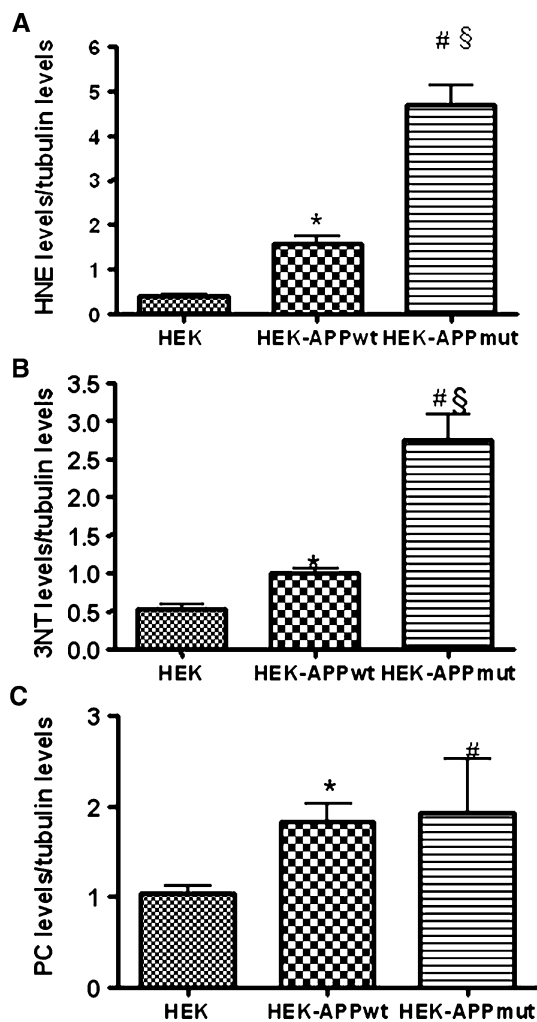
Fig. 4 Oxidative profile in HEK, HEK-APPwt and HEK-APPmut cells. Dot-blot analysis on protein extracts derived from HEK, HEK-APPwt and HEK-APPmut cells were performed using specific antibodies against oxidative stress markers: protein-bound HNE (**a**), 3NT (**b**) and PC (**c**). Tubulin expression was used to normalize the samples. Bars represented mean ± SEM of at least 3 different experiments. For protein-bound HNE levels: *$p < 0.01$ HEK-APPwt versus HEK, #$p < 0.001$ HEK-APPmut versus HEK; §$p < 0.001$ HEK-APPmut versus HEK-APPwt. For 3NT levels: *$p < 0.05$ HEK-APPwt versus HEK, #$p < 0.01$ HEK-APPmut versus HEK; §$p < 0.001$ HEK-APPmut versus HEK-APPwt. For PC levels: *$p < 0.05$ HEK-APPwt versus HEK, #$p < 0.05$ HEK-APPmut versus HEK

enzymes, before and after H_2O_2 treatment. SOD catalyses the dismutation of the superoxide anion into hydrogen peroxide and molecular oxygen (Maier and Chan 2002; Sultana et al. 2008). SOD activity in basal condition did not differ among the two clones and non-transfected cells. Figure 6, panel A, reported the percent increase of SOD activity after 1 h H_2O_2 exposure in the two APP clones and HEK cells. H_2O_2 treatment induced a 90% increase in SOD activity in HEK cells. Surprisingly, in HEK-APPwt cells, SOD activity increased by about 136% after 1 h H_2O_2

insult. In contrast, the APPmut clone responded to H_2O_2 increasing SOD activity by about 80% with respect to basal condition. The reduced induction of H_2O_2-triggered SOD activity found in HEK-APPmut cells, in comparison to HEK-APPwt, was associated with an increased H_2O_2-induced generation of oxidative stress. As shown in Fig. 6, panel B, the percentage increase of PC, HNE and 3NT markers induced by H_2O_2, was statistically higher in HEK-APPmut cells in comparison with those found in HEK-APPwt cells. At variance, HEK-APPwt clone appeared to be protected against oxidative stress injury, since oxidative markers resulted lower than those found in HEK cells after H_2O_2 exposure.

H_2O_2 exposure induced a fast increase of SOD1 expression, and a more delayed enhancement of SOD2 in HEK non-transfected cells (Fig. 6, panel C). In HEK-APPwt SOD1 expression was also rapidly induced by H_2O_2, however, it apparently declined already 1 h after the injury. On the other hand, SOD2 was activated very early after the lesion in HEK-APPwt clones. HEK-APPmut expressed, in basal condition high levels of SOD1 and SOD2 proteins, and after H_2O_2 treatment both SOD1 and SOD2 expression levels were found unchanged or even decreased.

Effects of soluble $A\beta_{1-40}$ and $A\beta_{1-42}$ on cell vulnerability, p53 conformational state and redox profile

We previously demonstrated that resistance to genotoxic insults and the p53 conformational changes in HEK-APPwt were mediated, at least in part, by $A\beta$ peptides (Uberti et al. 2007). Here, HEK cells were exposed to nanomolar concentration of both $A\beta_{1-40}$ and $A\beta_{1-42}$, and cell vulnerability, p53 conformational state and redox profile were evaluated. In particular, HEK cells were pre-treated for 48 h with $A\beta_{1-40}$ and $A\beta_{1-42}$ at different concentrations ranging from 0.02 to 10 nM, and then they were challenged with H_2O_2 as described in "Materials and methods" section. At any examined concentration both $A\beta_{1-40}$ and $A\beta_{1-42}$ protected the cells against oxidative insult (Fig. 7, panel A). Figure 7, panel B shows the effects of $A\beta$ peptides on p53 conformational state. HEK cells pre-treated with 10 nM $A\beta_{1-40}$ or $A\beta_{1-42}$ expressed a p53 isoform immunoreactive to PAb 240 antibody (unfolded p53), in addition to PAb 1620 positive p53 isoform (WT p53) (Fig. 7, panel B). $A\beta_{1-40}$ and $A\beta_{1-42}$ pre-treated cells were also evaluated in terms of ROS generation. Soluble $A\beta_{1-42}$ induced a 10% increase in ROS generation over the control at 24 h. In contrast, ROS generation induced by $A\beta_{1-40}$ was lower at least until 48 h (Fig. 7, panel C). Exposure to soluble nanomolar concentration of $A\beta_{1-40}$ and $A\beta_{1-42}$ did not influence SOD1 expression (Fig. 7, panel D). At variance SOD2 expression was found significantly enhanced in
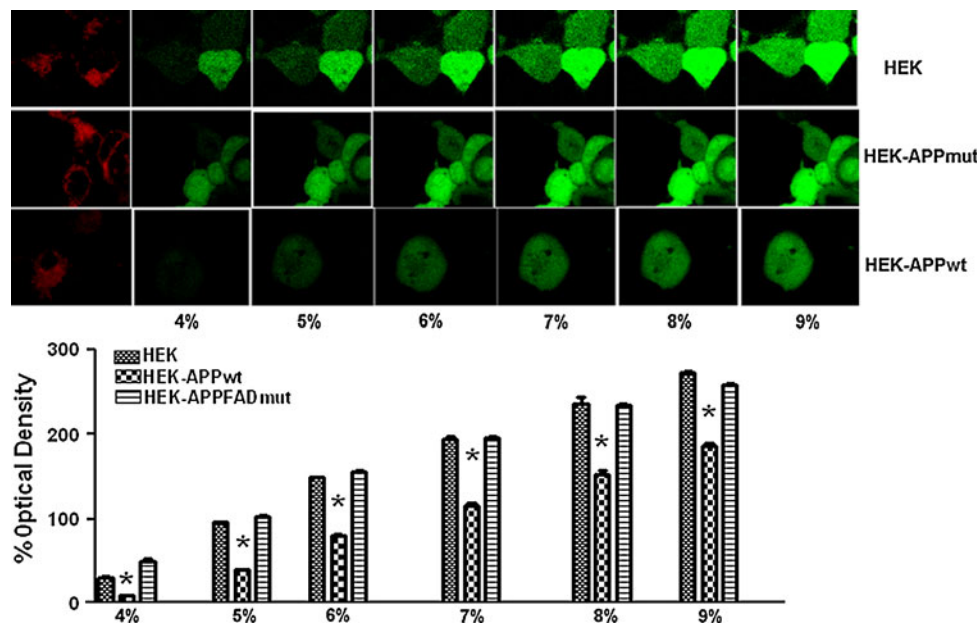
Fig. 5 Mitochondrial ROS levels in HEK, HEK-APPwt and HEK-APPmut. *Upper panel* using confocal microscopy technology, ROS production was followed during increased % of 488 nm laser intensity (*green*) in HEK, HEK-APPwt and HEK-APPmut living cells. Mitochondria were staining in *red* by using Mitotracker Deep Red 633 FM. *Lower panel* quantitative analysis of fluorescence intensity measured in HEK, HEK-APPwt and HEK-APPmut cells after different % of laser intensity. Data were expressed as % of optical density per pixel and corrected for background, and represent the mean value of at least three different cellular preparations. *$p < 0.01$ HEK-APPwt versus HEK and HEK-APPmut

$A\beta_{1-40}$ treated cells in comparison to those challenged with $A\beta_{1-42}$ peptide and untreated cells. On the other hand the total activity of SOD enzyme was found increased both in $A\beta_{1-40}$ and $A\beta_{1-42}$ treated cells in comparison with untreated cells, being $A\beta_{1-40}$ effects more pronounced than $A\beta_{1-42}$ (Fig. 7, panel D).

Discussion

Here, we show that overexpression of either wt or mut APP, although with a different degree, rescues the cells against H_2O_2-induced death. When comparing non-transfected cells with the two clones, it seems clear that the overexpression of wt or mut APP prevented H_2O_2 induced cell death. However, HEK-APPwt was more resistant to oxidative stress than HEK-APPmut. To better investigate such different behaviour in terms of H_2O_2-induced cell survival, the two cellular phenotypes were characterized in terms of $A\beta$ load, p53 intracellular signalling and oxidative profiles.

Overexpression of wt or mut APP induced an increased production of $A\beta$ peptides, in comparison with non-transfected cells. HEK-APPwt produced a large amount of $A\beta_{1-40}$, whereas the mutant clone expressed predominantly the 42 amino acids length peptide. These results are consistent with previous data indicating that the most

consistent effect of APP-related mutations was not a net gain of total $A\beta$ but rather an increase in the ratio of $A\beta_{1-42}/A\beta_{1-40}$ (Dutescu et al. 2009).

The first question arising from our finding is whether or not amyloid peptides, as APP metabolic products, were implicated in cell survival. Growing evidence suggests that $A\beta$ has important physiological roles and, at low levels, may even be crucial for cell survival (Kaltschmidt et al. 1999; Kuperstein et al. 2004; Goto et al. 2006; Pearson and Peers 2006; Tardito et al. 2007). That $A\beta$ peptides exert a survival role in specific cell phenotypes was demonstrated by Plant et al. (2003), who showed that, in primary cultures of central neurons and other neuronal cell lines, inhibition of endogenous $A\beta$ production, by exposure to inhibitors either of β or γ secretases, or immunodepletion of $A\beta$, caused neuronal death. Furthermore, nanomolar concentration of $A\beta_{1-40}$ was involved in endothelial cell survival, stimulating FGF2 mRNA and protein expression (Cantara et al. 2005). We also demonstrated that HEK cells exposed to 10 nM $A\beta_{1-40}$ protected cells against doxorubicin (Uberti et al. 2007). It is noteworthy that the majority of these studies have been performed by using the 1–40 amino acid length $A\beta$ peptide. Kim et al. (2007) with an elegant Tg mice model, in which mice that selectively expressed $A\beta_{1-40}$ were crossed with Tg mice expressing exclusively $A\beta_{1-42}$, demonstrated that $A\beta_{1-40}$ antagonized $A\beta_{1-42}$ effects. On the other hand, soluble nanomolar concentration
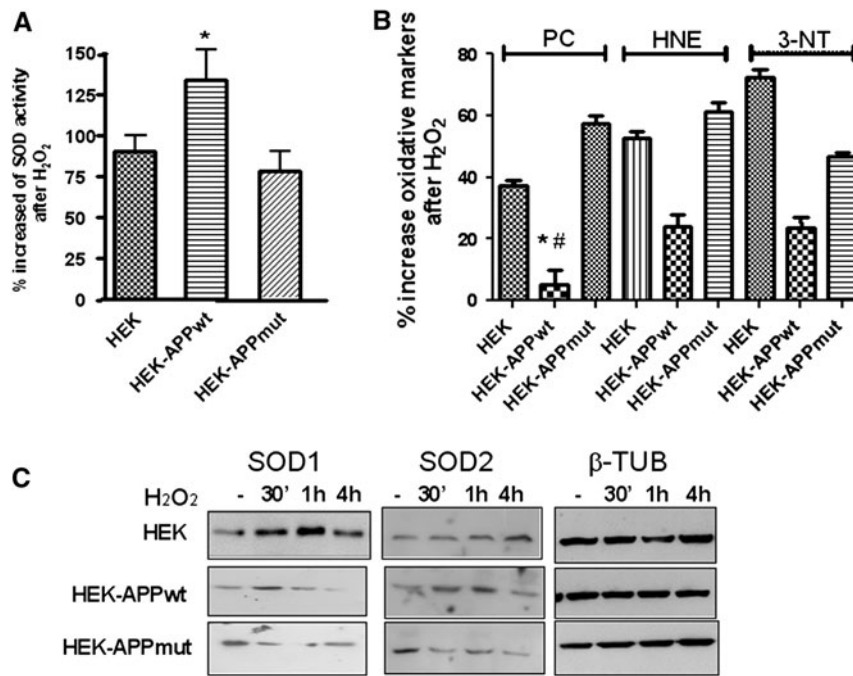
Fig. 6 Redox profile in HEK, HEK-APPwt and HEK-APPmut cells after oxidative insult. **a** The enzymatic activity of SOD, was measured in HEK, HEK-APPwt and HEK-APPmut cells in basal condition and after exposure to H_2O_2 using a specific assay (see "Materials and methods" section). Data were expressed as % increase of SOD activity after 1 h H_2O_2 treatment. $*p < 0.001$ HEK-APPwt versus HEK. **b** Dot-blot analysis with specific antibodies recognizing oxidative stress markers (HNE, 3NT and PC) in HEK, HEK-APPwt cells and HEK-APPmut cells before and after H_2O_2 pulse. Data were expressed as % increase of oxidative markers after 1 h H_2O_2 treatment. For protein-bound HNE levels: $*p < 0.01$ HEK-APPwt versus HEK, $^{\#}p < 0.001$ HEK-APPwt versus HEK-APPmut. For 3NT levels: $*p < 0.01$ HEK-APPwt versus HEK, $^{\#}p < 0.01$ HEK-APPwt versus HEK-APPmut. For PC levels: $*p < 0.01$ HEK-APPwt versus HEK, $^{\#}p < 0.05$ HEK-APPwt versus HEK-APPmut. **c** Western blotting analysis using anti-SOD1 and anti-SOD2 antibodies in HEK-APPwt, and HEK-APPFADmut, and HEK untransfected cells in basal conditions and after different time following H_2O_2 exposure. Tubulin expression was used to normalize the samples

of both $A\beta_{1-40}$ and $A\beta_{1-42}$ protected cells against oxidative injury, suggesting that, at least in a peripheral cellular model, the two peptides shared the same protective function. But, it is striking to remind that synthetic $A\beta_{1-40}$ and $A\beta_{1-42}$ peptides do not show all the properties of $A\beta$ peptides naturally generated in the brain (Shankar et al. 2007, 2008; Selkoe 2008).

Both HEK-APPwt and HEK-APPmut showed impairment in p53 intracellular signalling, as demonstrated by lack of p53 and p21/waf1 protein induction. This could be due to an altered conformational structure adopted by the protein in the two clones. These data confirmed our previous results in APP wt clone (Uberti et al. 2007), and gave new insight in the context of mutant APP. It appears that p53 belongs to a growing list of transcriptional activators which are post-transcriptionally regulated by redox modulation (Hainaut and Milner 1993; Sun and Oberley 1996; Verhaegh et al. 1997). In fact, as a result of protein oxidation, 9 out of the 12 cysteine residues in p53 localized in the central DNA-binding domain can be subjected to disulphide bound formation thus altering the tertiary structure of the protein. In this abnormal conformation,

p53 loses the capability to trans-activate its target genes (Parks et al. 1997). The conformational unfolded p53 found both in HEK-APPwt and in HEK-APPmut may explain the resistance of both cell clones to oxidative insult. Similarly $A\beta_{1-40}$ and $A\beta_{1-42}$ treatments induced p53 conformational changes on HEK cells, suggesting that among APP metabolic products, the short peptides seemed to be those mainly involved. On the other hand the involvement of the other APP metabolic products, such as sAPPα, on p53 conformational changes was previously excluded (Uberti et al. 2007). Furthermore, $A\beta$ peptides have been found to induce p53 conformational changes in many cell phenotypes, such as fibroblast (Lanni et al. 2007), neuroblastoma cells and also cortical neurons (data not shown). It is well known that $A\beta$ itself is pro-oxidant (Butterfield 1997; Boyd-Kimball et al. 2005; Cenini et al. 2009) and we also demonstrated that especially $A\beta_{1-42}$ induced ROS generation in vitro.

Thus, we hypothesised that, if APP amyloidogenic products have a role in inducing p53 conformational changes, they may influence, directly or indirectly, the redox state of the protein.
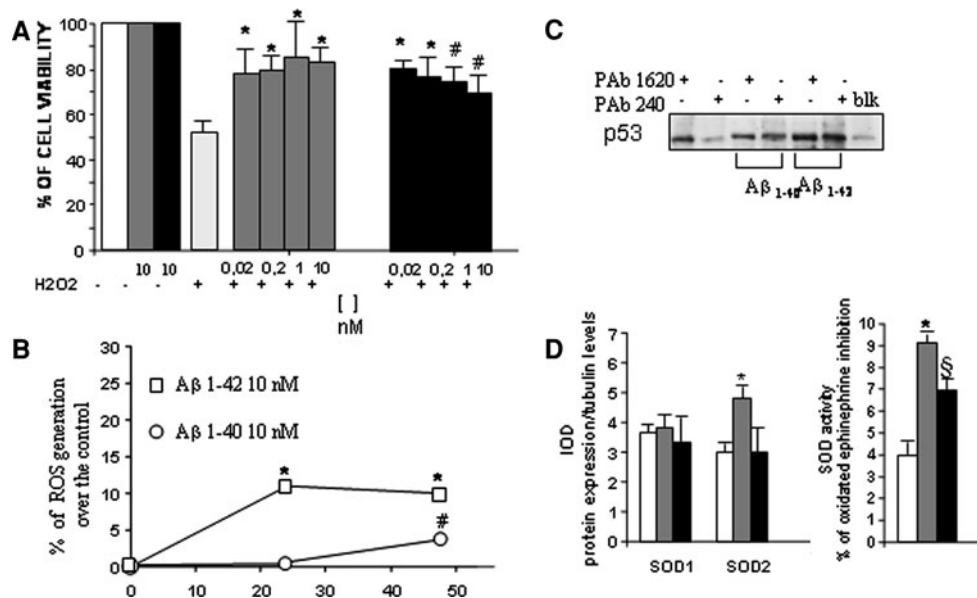
Fig. 7 Effects of Aβ$_{1-40}$ and Aβ$_{1-42}$ on cell vulnerability against oxidative injury, p53 conformational state and redox profile. **a** HEK cells were pre-treated with different nanomolar concentration of Aβ$_{1-40}$ (*grey bar*) and Aβ$_{1-42}$ (*black bar*) and then challenged with H$_2$O$_2$ pulse. After 24 h cell vulnerability was measured by MTT assay. The data were expressed as % of cell survival versus control. *$p < 0.05$ versus the corresponding control values, #$p < 0.01$ versus the corresponding control values. **b** Protein extracts derived from HEK cell treated for 48 h with Aβ$_{1-40}$ or Aβ$_{1-42}$ were immunoprecipitated with the following antibodies: PAb240 (specific for "mutant" unfolded conformation) and PAb1620 (specific for wild-

type folded conformation). Immunoprecipitates were analysed by Western blot with the CM1 polyclonal anti-p53 antibody. **c** ROS generation inside the cells was measured using DCF fluorescence 24 and 48 h after Aβ$_{1-40}$ (*circle*) and Aβ$_{1-42}$ (*square*) treatment. Data represent means ± SEM of at least three different experiments from three separate cell preparations. *$p < 0.001$ versus the corresponding control values, #$p < 0.01$ versus the corresponding control values. **d** Quantitative analysis of SOD1 and SOD2 expression and SOD activity after Aβ$_{1-40}$ and Aβ$_{1-42}$ treatment. *$p < 0.001$ Ab 1–40 treated versus untreated cells; *$p < 0.01$ Ab 1–42 treated versus untreated cells

To figure out whether unfolded p53 isoform was the result of oxidative environment, the redox profiles of HEK-APPwt and HEK-APPmut were studied. Measurement of oxidative markers pointed out some differences between HEK-APPwt and HEK-APPmut. Although protein-bound HNE, 3NT and PC markers were increased both in HEK-APPwt and in HEK-APPmut in comparison with HEK non-transfected cells, the levels of oxidative stress in the mutant clone was higher than those found in HEK-APPwt. In particular, HNE Michael adducts, products of lipid peroxidation, and 3NT, products of nitrosylation, were found statistically enhanced in HEK-APPmut cells, in comparison with HEK-APPwt. These data matched well with the findings observed in mitochondria. Evaluating living single cells, by confocal microscopy, during increasing laser intensity (that resembled an oxidative stress injury) (Bassoe et al. 2003), an higher increase in ROS production inside mitochondria was reported in HEK-APPmut cells in comparison with those found in HEK-APPwt cells. Already at 4% laser exposure, that represents the basal condition, an increase in ROS production was found in cells overexpressing APPmut in comparison with HEK-APPwt cells. Furthermore, mitochondrial ROS generation in HEK-APPwt were even lower than that measured in HEK non-transfected cells. These

findings suggest that HEK-APPwt cells were, in some way, more protected against oxidative stress. Aβ$_{1-40}$ and Aβ$_{1-42}$-induced ROS generation could resemble what we observed, respectively, in HEK-APPwt with Aβ$_{1-42}$/Aβ$_{1-40}$ ratio of 0,41 pg/mg and HEK-APPmut with Aβ$_{1-42}$/Aβ$_{1-40}$ ratio of 1.3 pg/mg.

Oxidative stress develops when the well-regulated balance between pro-oxidants and antioxidants gets out of control in favour of the pro-oxidants (Harman 1988, 2006). In our experimental models total SOD activity was not dramatically different in two clones and non-transfected cells. Surprisingly, when cells were exposed to an oxidative injury, an increased SOD activity was observed in HEK-APPwt cells, but not in HEK-APPmut, in comparison with control cells. Differently both Aβ$_{1-40}$ and Aβ$_{1-42}$ treatments induced a significant increase in SOD activity, with Aβ$_{1-40}$ being more efficient in inducing this effect. The differences observed in HEK cells overexpressing APPwt and APPmut and synthetic Aβ peptide treatments can be attributed to establishment of compensatory responses occurring in stable transfected clones. Moreover, in HEK-APPwt, mitochondrial SOD2 protein levels were induced very rapidly, already 30 min after H$_2$O$_2$ exposure, thus explaining the lower ROS production in mitochondria

after exposure to laser stimulation, and the less sensitivity to oxidative injury in comparison with HEK-APPmut and non-transfected cells. At this regards, different studies (Huang et al. 1997; Kasahara et al. 2005; Takada et al. 2009) have correlated high expression of SOD2 with cell survival. SOD2 as well as SOD1 expressions were already high in basal condition in HEK-APPmut. This could be related to the high levels of oxidative stress that this clone expressed. However, when an acute oxidative injury occurs SOD protein levels did not change or even decrease in HEK-APPmut. It is noteworthy that $A\beta_{1-40}$, but not $A\beta_{1-42}$, exposure increased SOD2 expression. Differently both $A\beta_{1-40}$ and $A\beta_{1-42}$ peptides did not essentially modify the expression of SOD1 proteins in comparison with untreated cells. These results suggested that the increased SOD activity induced by and $A\beta_{1-42}$ peptides did not necessarily require protein transcription. On the other hand the effects of $A\beta_{1-40}$ on SOD2 expression seems to resemble what was observed in HEK-APPwt clone.

According to "hormesis theory" (Calabrese and Baldwin 1998; Toussaint et al. 2002), sub-lethal exposure to stressors induces a compensatory adaptive response that results in stress resistance. At this regard, it has been shown that when cells are exposed repeatedly to low doses of H_2O_2, they became resistant towards subsequent higher amount of ROS that would be lethal without pre-treatment (Janssen et al. 1993). In our model (HEK-APPwt cells), low amount of oxidative stress, as that found in basal condition, may exert a beneficial effect that at a higher intensity results harmful. In this condition, all antioxidant systems are alerted, and when an acute injury occurs, they are soon ready to act. At variance, HEK-APPmut cells lose this stress resistance probably because the degree of oxidative stress is too high and antioxidant enzymes are already compromised.

References

Alexandratou E, Yova D, Loukas S (2005) A confocal microscopy study of the very early cellular response to oxidative stress induced by zinc phthalocyanine sensitization. Free Radic Biol Med 39:1119–1127

Bassoe CF, Li N, Ragheb K, Lawler G, Sturgis J, Robinson JP (2003) Investigations of phagosomes, mitochondria, and acidic granules in human neutrophils using fluorescent probes. Cytometry B Clin Cytom 51:21–29

Beer J, Masters CL, Beyreuther K (1995) Cells from peripheral tissues that exhibit high APP expression are characterized by their high membrane fusion activity. Neurodegeneration 4:51–59

Boyd-Kimball D, Sultana R, Mohmmad-Abdul H, Butterfield DA (2005) Neurotoxicity and oxidative stress in D1M-substituted Alzheimer's A beta(1–42): relevance to N-terminal methionine chemistry in small model peptides. Peptides 26:665–673

Butterfield DA (1997) Beta-amyloid-associated free radical oxidative stress and neurotoxicity: implications for Alzheimer's disease. Chem Res Toxicol 10:495–506

Butterfield DA, Stadtman ER (1997) Protein oxidation processes in aging brain. Adv Cell Aging Gerontol 2:161–191

Butterfield DA, Castegna A, Lauderback CM, Drake J (2002) Evidence that amyloid beta-peptide-induced lipid peroxidation and its sequelae in Alzheimer's disease brain contribute to neuronal death. Neurobiol Aging 23:655–664

Butterfield DA, Reed T, Perluigi M, De Marco C, Coccia R, Cini C, Sultana R (2006) Elevated protein-bound levels of the lipid peroxidation product, 4-hydroxy-2-nonenal, in brain from persons with mild cognitive impairment. Neurosci Lett 397:170–173

Calabrese EJ, Baldwin LA (1998) Hormesis as a biological hypothesis. Environ Health Perspect 106(Suppl 1):357–362

Cantara S, Donnini S, Morbidelli L, Giachetti A, Schulz R, Memo M, Ziche M (2004) Physiological levels of amyloid peptides stimulate the angiogenic response through FGF-2. Faseb J 18:1943–1945

Cantara S, Ziche M, Donnini S (2005) Opposite effects of beta amyloid on endothelial cell survival: role of fibroblast growth factor-2 (FGF-2). Pharmacol Rep 57(Suppl):138–143

Castegna A, Thongboonkerd V, Klein JB, Lynn B, Markesbery WR, Butterfield DA (2003) Proteomic identification of nitrated proteins in Alzheimer's disease brain. J Neurochem 85:1394–1401

Cenini G, Cecchi C, Pensalfini A, Bonini SA, Ferrari-Toninelli G, Liguri G, Memo M, Uberti D (2009) Generation of reactive oxygen species by beta amyloid fibrils and oligomers involves different intra/extracellular pathways. Amino acids [Epub ahead of print]

De Strooper B, Annaert W (2000) Proteolytic processing and cell biological functions of the amyloid precursor protein. J Cell Sci 113(Pt 11):1857–1870

Drake J, Sultana R, Aksenova M, Calabrese V, Butterfield DA (2003) Elevation of mitochondrial glutathione by gamma-glutamylcysteine ethyl ester protects mitochondria against peroxynitrite-induced oxidative stress. J Neurosci Res 74:917–927

Dugan LL, Sensi SL, Canzoniero LM, Handran SD, Rothman SM, Lin TS, Goldberg MP, Choi DW (1995) Mitochondrial production of reactive oxygen species in cortical neurons following exposure to N-methyl-D-aspartate. J Neurosci 15:6377–6388

Dutescu RM, Li QX, Crowston J, Masters CL, Baird PN, Culvenor JG (2009) Amyloid precursor protein processing and retinal pathology in mouse models of Alzheimer's disease. Graefes Arch Clin Exp Ophthal 247:1213–1221

Gansauge S, Gansauge F, Gause H, Poch B, Schoenberg MH, Beger HG (1997) The induction of apoptosis in proliferating human fibroblasts by oxygen radicals is associated with a p53- and p21WAF1CIP1 induction. FEBS Lett 404:6–10

Goto Y, Niidome T, Akaike A, Kihara T, Sugimoto H (2006) Amyloid beta-peptide preconditioning reduces glutamate-induced neurotoxicity by promoting endocytosis of NMDA receptor. Biochem Biophys Res Commun 351:259–265

Graebert KS, Lemansky P, Kehle T, Herzog V (1995) Localization and regulated release of Alzheimer amyloid precursor-like protein in thyrocytes. Lab Invest 72:513–523

Grimm MO, Grimm HS, Hartmann T (2007) Amyloid beta as a regulator of lipid homeostasis. Trends Mol Med 13:337–344

Gutteridge JM, Halliwell B (2000) Free radicals and antioxidants in the year 2000. A historical look to the future. Ann N Y Acad Sci 899:136–147

Hainaut P, Milner J (1993) Redox modulation of p53 conformation and sequence-specific DNA binding in vitro. Cancer Res 53:4469–4473

Halliwell B (2007) Biochemistry of oxidative stress. Biochem Soc Trans 35:1147–1150

Halliwell B (2009) The wanderings of a free radical. Free Radic Biol Med 46:531–542

Harman D (1988) Free radicals in aging. Mol Cell Biochem 84:155–161

Harman D (2006) Free radical theory of aging: an update: increasing the functional life span. Ann N Y Acad Sci 1067:10–21

Herzog V, Kirfel G, Siemes C, Schmitz A (2004) Biological roles of APP in the epidermis. Eur J Cell Biol 83:613–624

Huang TT, Yasunami M, Carlson EJ, Gillespie AM, Reaume AG, Hoffman EK, Chan PH, Scott RW, Epstein CJ (1997) Superoxide-mediated cytotoxicity in superoxide dismutase-deficient fetal fibroblasts. Arch Biochem Biophys 344:424–432

Janssen YM, Van Houten B, Borm PJ, Mossman BT (1993) Cell and tissue responses to oxidative damage. Lab Invest 69:261–274

Johnson TM, Yu ZX, Ferrans VJ, Lowenstein RA, Finkel T (1996) Reactive oxygen species are downstream mediators of p53-dependent apoptosis. Proc Natl Acad Sci USA 93:11848–11852

Kaltschmidt B, Uherek M, Wellmann H, Volk B, Kaltschmidt C (1999) Inhibition of NF-kappaB potentiates amyloid beta-mediated neuronal apoptosis. Proc Natl Acad Sci USA 96:9409–9414

Kasahara E, Lin LR, Ho YS, Reddy VN (2005) SOD2 protects against oxidation-induced apoptosis in mouse retinal pigment epithelium: implications for age-related macular degeneration. Invest Ophthalmol Vis Sci 46:3426–3434

Kim J, Onstead L, Randle S, Price R, Smithson L, Zwizinski C, Dickson DW, Golde T, McGowan E (2007) Abeta40 inhibits amyloid deposition in vivo. J Neurosci 27:627–633

Knobloch M, Mansuy IM (2008) Dendritic spine loss and synaptic alterations in Alzheimer's disease. Mol Neurobiol 37:73–82

Kuperstein F, Brand A, Yavin E (2004) Amyloid Abeta1–40 preconditions non-apoptotic signals in vivo and protects fetal rat brain from intrauterine ischemic stress. J Neurochem 91:965–974

Kweon SM, Kim HJ, Lee ZW, Kim SJ, Kim SI, Paik SG, Ha KS (2001) Real-time measurement of intracellular reactive oxygen species using Mito tracker orange (CMH2TMRos). Biosci Rep 21:341–352

LaFerla FM, Green KN, Oddo S (2007) Intracellular amyloid-beta in Alzheimer's disease. Nat Rev Neurosci 8:499–509

Lanni C, Uberti D, Racchi M, Govoni S, Memo M (2007) Unfolded p53: a potential biomarker for Alzheimer's disease. J Alzheimers Dis 12:93–99

Lauderback CM, Hackett JM, Huang FF, Keller JN, Szweda LI, Markesbery WR, Butterfield DA (2001) The glial glutamate transporter, GLT-1, is oxidatively modified by 4-hydroxy-2-nonenal in the Alzheimer's disease brain: the role of Abeta1–42. J Neurochem 78:413–416

Maier CM, Chan PH (2002) Role of superoxide dismutases in oxidative damage and neurodegenerative disorders. Neuroscientist 8:323–334

Markesbery WR, Lovell MA (1998) Four-hydroxynonenal, a product of lipid peroxidation, is increased in the brain in Alzheimer's disease. Neurobiol Aging 19:33–36

Nakamura T, Sakamoto K (2001) Reactive oxygen species upregulates cyclooxygenase-2, p53, and Bax mRNA expression in bovine luteal cells. Biochem Biophys Res Commun 284:203–210

Parks D, Bolinger R, Mann K (1997) Redox state regulates binding of p53 to sequence-specific DNA, but not to non-specific or mismatched DNA. Nucleic Acids Res 25:1289–1295

Pearson HA, Peers C (2006) Physiological roles for amyloid beta peptides. J Physiol 575:5–10

Perluigi M, Joshi G, Sultana R, Calabrese V, De Marco C, Coccia R, Cini C, Butterfield DA (2006) In vivo protective effects of ferulic acid ethyl ester against amyloid-beta peptide 1–42-induced oxidative stress. J Neurosci Res 84:418–426

Plant LD, Boyle JP, Smith IF, Peers C, Pearson HA (2003) The production of amyloid beta peptide is a critical requirement for the viability of central neurons. J Neurosci 23:5531–5535

Saitoh T, Sundsmo M, Roch JM, Kimura N, Cole G, Schubert D, Oltersdorf T, Schenk DB (1989) Secreted form of amyloid beta protein precursor is involved in the growth regulation of fibroblasts. Cell 58:615–622

Schmitz A, Tikkanen R, Kirfel G, Herzog V (2002) The biological role of the Alzheimer amyloid precursor protein in epithelial cells. Histochem Cell Biol 117:171–180

Selkoe DJ (2008) Soluble oligomers of the amyloid beta-protein impair synaptic plasticity and behavior. Behav Brain Res 192:106–113

Shankar GM, Bloodgood BL, Townsend M, Walsh DM, Selkoe DJ, Sabatini BL (2007) Natural oligomers of the Alzheimer amyloid-beta protein induce reversible synapse loss by modulating an NMDA-type glutamate receptor-dependent signaling pathway. J Neurosci 27:2866–2875

Shankar GM, Li S, Mehta TH, Garcia-Munoz A, Shepardson NE, Smith I, Brett FM, Farrell MA, Rowan MJ, Lemere CA, Regan CM, Walsh DM, Sabatini BL, Selkoe DJ (2008) Amyloid-beta protein dimers isolated directly from Alzheimer's brains impair synaptic plasticity and memory. Nat Med 14:837–842

Sultana R, Butterfield DA (2008) Slot-blot analysis of 3-nitrotyrosine-modified brain proteins. Methods Enzymol 440:309–316

Sultana R, Poon HF, Cai J, Pierce WM, Merchant M, Klein JB, Markesbery WR, Butterfield DA (2006a) Identification of nitrated proteins in Alzheimer's disease brain using a redox proteomics approach. Neurobiol Dis 22:76–87

Sultana R, Boyd-Kimball D, Poon HF, Cai J, Pierce WM, Klein JB, Merchant M, Markesbery WR, Butterfield DA (2006b) Redox proteomics identification of oxidized proteins in Alzheimer's disease hippocampus and cerebellum: an approach to understand pathological and biochemical alterations in AD. Neurobiol Aging 27:1564–1576

Sultana R, Piroddi M, Galli F, Butterfield DA (2008) Protein levels and activity of some antioxidant enzymes in hippocampus of subjects with amnestic mild cognitive impairment. Neurochem Res 33:2540–2546

Sultana R, Newman SF, Huang Q, Butterfield DA (2009) Detection of carbonylated proteins in two-dimensional sodium dodecyl sulfate polyacrylamide gel electrophoresis separations. Methods Mol Biol 476:149–159

Sun Y, Oberley LW (1996) Redox regulation of transcriptional activators. Free Radic Biol Med 21:335–348

Takada S, Inoue E, Tano K, Yoshii H, Abe T, Yoshimura A, Akita M, Tada S, Watanabe M, Seki M, Enomoto T (2009) Generation and characterization of cells that can be conditionally depleted of mitochondrial SOD2. Biochem Biophys Res Commun 379:233–238

Tardito D, Gennarelli M, Musazzi L, Gesuete R, Chiarini S, Barbiero VS, Rydel RE, Racagni G, Popoli M (2007) Long-term soluble Abeta1–40 activates CaM kinase II in organotypic hippocampal cultures. Neurobiol Aging 28:1388–1395

Thinakaran G, Koo EH (2008) Amyloid precursor protein trafficking, processing, and function. J Biol Chem 283:29615–29619

Toussaint O, Remacle J, Dierick JF, Pascal T, Frippiat C, Royer V, Chainiaux F (2002) Approach of evolutionary theories of ageing, stress, senescence-like phenotypes, calorie restriction and hormesis from the view point of far-from-equilibrium thermodynamics. Mech Ageing Dev 123:937–946

Uberti D, Yavin E, Gil S, Ayasola KR, Goldfinger N, Rotter V (1999) Hydrogen peroxide induces nuclear translocation of p53 and apoptosis in cells of oligodendroglia origin. Brain Res Mol Brain Res 65:167–175

Uberti D, Carsana T, Bernardi E, Rodella L, Grigolato P, Lanni C, Racchi M, Govoni S, Memo M (2002) Selective impairment of p53-mediated cell death in fibroblasts from sporadic Alzheimer's disease patients. J Cell Sci 115:3131–3138

Uberti D, Cenini G, Olivari L, Ferrari-Toninelli G, Porrello E, Cecchi C, Pensalfini A, Liguri G, Govoni S, Racchi M, Maurizio M (2007) Over-expression of amyloid precursor protein in HEK cells alters p53 conformational state and protects against doxorubicin. J Neurochem 103:322–333

Uchida K (2003) 4-Hydroxy-2-nonenal: a product and mediator of oxidative stress. Prog Lipid Res 42:318–343

Valko M, Leibfritz D, Moncol J, Cronin MT, Mazur M, Telser J (2007) Free radicals and antioxidants in normal physiological functions and human disease. Int J Biochem Cell Biol 39:44–84

Verhaegh GW, Richard MJ, Hainaut P (1997) Regulation of p53 by metal ions and by antioxidants: dithiocarbamate down-regulates p53 DNA-binding activity by increasing the intracellular level of copper. Mol Cell Biol 17:5699–5706

Vetrivel KS, Thinakaran G (2006) Amyloidogenic processing of beta-amyloid precursor protein in intracellular compartments. Neurology 66:S69–S73

Walsh DM, Selkoe DJ (2007) A beta oligomers—a decade of discovery. J Neurochem 101:1172–1184

Walsh DM, Minogue AM, Sala Frigerio C, Fadeeva JV, Wasco W, Selkoe DJ (2007) The APP family of proteins: similarities and differences. Biochem Soc Trans 35:416–420

Xu X, Yang D, Wyss-Coray T, Yan J, Gan L, Sun Y, Mucke L (1999) Wild-type but not Alzheimer-mutant amyloid precursor protein confers resistance against p53-mediated apoptosis. Proc Natl Acad Sci USA 96:7547–7552